Journal of Solid State Chemistry 184 (2011) 1451–1458

Contents lists available at ScienceDirect

Journal of Solid State Chemistry

journal homepage: www.elsevier.com/locate/jssc

Effect of lanthanide contraction on the mixed polyamine systems Ln/Sb/Se/(en+dien) and Ln/Sb/Se/(en+trien): Syntheses and characterizations of lanthanide complexes with a tetraselenidoantimonate ligand

Jing Zhao, Jingjing Liang, Yingli Pan, Yong Zhang, Dingxian Jia *

Key Laboratory of Organic Synthesis of Jiangsu Province, College of Chemistry, Chemical Engineering and Materials Science, Dushu Lake Campus, Soochow University, No. 199 Hengyi Road, Suzhou 215123, People's Republic of China

ARTICLE INFO

Article history:
Received 16 November 2010
Received in revised form
15 March 2011
Accepted 21 March 2011
Available online 19 April 2011

Keywords:
Selenidoantimonate ligand
Lanthanide
Solvothermal synthesis
Structure elucidation
Optical properties

ABSTRACT

Mixed polyamine systems Ln/Sb/Se/(en+dien) and Ln/Sb/Se/(en+trien) (Ln=lanthanide, en=ethylenediamine, dien=diethylenetriamine, trien=triethylenetetramine) were investigated under solvothermal conditions, and novel mixed-coordinated lanthanide(III) complexes $[Ln(en)_2(dien)(\eta^2\text{-}SbSe_4)]$ (*Ln*=Ce(**1a**), Nd(**1b**)), $[Ln(en)_2(dien)(SbSe_4)]$ (*Ln*=Sm(**2a**), Gd(**2b**), Dy(**2c**)), $[Ln(en)(trien)(\mu\text{-}\eta^1,\eta^2\text{-}SbSe_4)]_\infty$ (*Ln*=Ce(**3a**), Nd(**3b**)) and $[Sm(en)(trien)(\eta^2\text{-}SbSe_4)]$ (**4a**) were prepared. Two structural types of lanthanide selenidoantimonates were obtained across the lanthanide series in both en+dien and en+trien systems. The tetrahedral anion $[SbSe_4]^{3-}$ acts as a monodentate ligand *mono*-$SbSe_4$, a bidentate chelating ligand η^2-$SbSe_4$ or a tridentate bridging ligand μ-η^1,η^2-$SbSe_4$ to the lanthanide(III) center depending on the Ln^{3+} ions and the mixed ethylene polyamines, indicating the effect of lanthanide contraction on the structures of the lanthanide(III) selenidoantimonates. The lanthanide selenidoantimonates exhibit semiconducting properties with E_g between 2.08 and 2.51 eV.

1. Introduction

Solvothermal reactions in polyamine solvents have proven to be a fruitful approach to the synthesis of main group chalcogenidometalates combining with transition–metal (TM) complexes, and a large number of these TM containing chalcogenidometalates, including chalcogenido-germanates [1], -stannates [2], -arsenates [3], and -antimonates [4] have been synthesized in polyamine solvents of ethylenediamine (en) and diethylenetriamine (dien). Besides being the reaction solvents, the polyamine molecules also act as chelating ligands to coordinate to TM^{n+} to form the complex cations $[TM(polyamine)_m]^{n+}$, which act as space fillers and/or charge compensating ions in the chalcogenidometalates. However, the incorporation of TM^{n+} centers in chalcogenidometalate networks is seldom observed in en and dien, because the coordinate sites of TM^{n+} ions are prone to being saturated by the bidentate en and tridentate dien ligands due to the formation of octahedral complexes $[TM(en)_3]^{n+}$ and $[TM(dien)_2]^{n+}$. The TM coordinated chalcogenidometalates are only observed for Cr^{3+} and Mn^{2+} metals, including the limited examples of $[Cr(en)_2(GeS_4)]^-$, $[\{Cr(en)\}_2(GeSe_4)_2]^{2-}$, $[Cr(en)_2(SnSe_4)]^-$ [5], $[\{Mn(en)_2\}_2(en)(Sn_2S_6)]$ [6], $[Mn(dien)(AsS_4)]^-$ [7], $Cr(en)_2SbS_3$ [8], $[Mn_2(en)_2(Sb_2S_5)]$ [9], $[Mn_2(dien)(Sb_2S_5)]$ [10], $[Mn_4(en)_9(SbSe_4)_4]^{4-}$ [11], and $[Mn_2(SbSe_4)_2(en)_4(H_2O)]^{2-}$ [12]. The effective incorporation of TM into chalcogenidometalate anions is well achieved by adopting the tetradentate polyamine, tris(2-aminoethyl)amine (tren), and pentadentate polyamine, tetraethylenepentamine (tepa), as structure directing agents. The TM^{n+} ion is then coordinated by a tren or tepa ligand and leaves one or two coordination sites free for TM–S or TM–Se bond formation with the chalcogenidometalate anions. Indeed, a large number of chalcogenidometalates incorporated with TM complexes of Mn^{2+}, Fe^{2+}, Co^{2+}, and Ni^{2+} have been prepared with tren [13] and tepa [14] as the chelating ligands of TM^{n+}.

Unlike the TM^{n+} metals which exhibit the restricted stereochemistry in coordination complexes, the lanthanide (Ln) ions are characterized by variable coordination numbers and geometries [15], which theoretically provides the Ln^{3+} ions with different structural features from the TM^{n+} ions in the combination with chalcogenidometalate anionic ligands in the presence of ethylene polyamines. In recent years, we investigated the solvothermal synthetic systems Ln/*M*/*Q* (Ln=lanthanide; *M*=Sn, As, Sb; *Q*=S, Se) in en and dien, and prepared a series of lanthanide-containing chalcogenidometalates. In these lanthanide chalcogenidometalates the coordination of $[SnSe_4]^{4-}$, $[Sn_2Se_6]^{4-}$, $[Sn_4Se_9]^{6-}$ [16], $[AsSe_4]^{3-}$ [17], $[SbS_4]^{3-}$ [18], and $[SbSe_4]^{3-}$ [19,20] anions to the Ln^{3+}-en and Ln^{3+}-dien unsaturated complexes have been successfully achieved. In the case

* Corresponding author. Fax: +86 512 65880089.
E-mail address: jiadingxian@suda.edu.cn (D. Jia).

0022-4596/$ - see front matter © 2011 Elsevier Inc. All rights reserved.
doi:10.1016/j.jssc.2011.03.039

of the Ln/Sb/Se/en system, [*Ln*(en)$_4$(SbSe$_4$)] (*Ln*=La, Ce, Pr, and Nd) and [*Ln*(en)$_4$]SbSe$_4\cdot$0.5en (*Ln*=Eu, Gd, Er, Tm, and Yb) two structural types are formed along the lanthanide series [19]. In the present work, the mixed polyamine systems Ln/Sb/Se/(en+dien) and Ln/Sb/Se/(en+trien) are explored in detail across the lanthanide series to elucidate the lanthanide contraction effect on the structures, and neutral selenidoantimonates containing lanthanide(III) complexes of mixed ethylene polyamine ligands, [*Ln*(en)$_2$(dien)(η^2-SbSe$_4$)] (*Ln*=Ce(**1a**), Nd(**1b**)), [*Ln*(en)$_2$(dien)(SbSe$_4$)] (*Ln*=Sm(**2a**), Gd(**2b**), Dy(**2c**)), [*Ln*(en)(trien)(μ-η^1,η^2-SbSe$_4$)]$_\infty$ (*Ln*=Ce(**3a**), Nd(**3b**)) and [Sm(en)(trien)(η^2-SbSe$_4$)] (**4a**), were prepared and characterized.

2. Experimental section

2.1. Materials and physical measurements

All the solvents and reagents for synthesis were commercially available and used as purchased. Elemental analyses were performed on a EA1110-CHNS–O elemental analyzer. Room-temperature optical diffuse reflectance spectra of the powdered sample were obtained with a Shimadzu UV-3150 spectrometer. The absorption (α/S) data were calculated from the reflectance using the Kubelka–Munk function $\alpha/S=(1-R)^2/2R$ [21], where R is the reflectance at a given energy, α is the absorption, and S is the scattering coefficient.

2.2. Synthesis of [Ln(en)$_2$(dien)(η^2-SbSe$_4$)] (Ln=Ce(**1a**), Nd(**1b**)) and [Ln(en)$_2$(dien)(SbSe$_4$)] (Ln=Sm(**2a**), Gd(**2b**), Dy(**2c**))

$CeCl_3$ (123 mg, 0.5 mmol), Sb (61 mg, 0.5 mmol), Se (158 mg, 2 mmol), and 2 mL of a mixed en/dien (1:1(v/v)) solvent were loaded into a Teflon-lined stainless steel autoclave with an inner volume of 15 mL. The reaction was run at 180 °C for 6 days, then cooled to ambient temperature. Yellow chip crystals of **1a** were filtered off, washed with ethanol and stored under vacuum (61% yield based on Sb). Red crystals of **1b** (57% yield), orange crystals of **2a** (48% yield), orange crystals of **2b** (49% yield) and red crystals of **2c** (45% yield) were prepared with a procedure similar to that for the synthesis of **1a**, except that Nd_2O_3, Sm_2O_3, Gd_2O_3, and Dy_2O_3 were used instead of $CeCl_3$, respectively. All the samples are stable in dry air. Anal. Found: C 11.85, H 3.57, N 12.12. Calcd. for $C_8H_{29}N_7Se_4CeSb$ (**1a**, 801.09): C 11.99, H 3.65, N 12.24%. Anal. Found: C 11.78, H 3.52, N 12.09. Calcd. for $C_8H_{29}N_7Se_4NdSb$ (**1b**, 805.21): C 11.93, H 3.63, N 12.18%. Anal. Found: C 11.70, H 3.51, N 11.95. Calcd. for $C_{16}H_{58}N_{14}Se_8Sm_2Sb_2$ (**2a**, 1622.64): C 11.84, H 3.60, N 12.08%. Anal. Found: 11.71, H 3.50, N 11.84. Calcd. for $C_{16}H_{58}N_{14}Se_8Gd_2Sb_2$ (**2b**, 1636.44): C 11.74, H 3.57, N 11.98%.

Table 1
Crystallographic data for **1a**−**4a**.

	1a	**1b**	**2a**	**2b**
Empirical formula	$C_8H_{29}N_7Se_4CeSb$	$C_8H_{29}N_7Se_4NdSb$	$C_{16}H_{58}N_{14}Se_8Sm_2Sb_2$	$C_{16}H_{58}N_{14}Se_8Gd_2Sb_2$
Formula weight	801.09	805.21	1622.64	1636.44
Cryst syst	Monoclinic	Monoclinic	Triclinic	Triclinic
Space group	$P2_1/n$	$P2_1/n$	$P-1$	$P-1$
a (Å)	8.6448(13)	8.6186(14)	10.037(3)	10.121(2)
b (Å)	27.844(4)	27.777(4)	12.117(3)	12.092(3)
c (Å)	9.3387(14)	9.3125(15)	17.125(4)	17.189(4)
α (deg)	90	90	88.888(9)	89.102(10)
β (deg)	109.086(2)	109.211(3)	88.651(9)	88.438(9)
γ (deg)	90	90	86.658(9)	86.889(10)
V (Å^3)	2124.3(5)	2105.3(6)	2078.2(9)	2099.6(8)
Z	4	4	2	2
T (K)	223(2)	293(2)	223(2)	293(2)
$D_{calcd.}$ (g cm^{-3})	2.505	2.540	2.593	2.589
Total, unique data	11 553, 4842	20 384, 3855	19 802, 7260	20 158, 7646
Parameters	191	191	371	374
R_1 ($I>2\sigma$ (I))	0.0383	0.0421	0.0481	0.0595
wR_2 (all data)	0.0743	0.0845	0.1382	0.1945
GOF on F^2	1.061	1.161	1.121	1.128
	2c	**3a**	**3b**	**4a**
Empirical formula	$C_{16}H_{58}N_{14}Se_8Dy_2Sb_2$	$C_8H_{26}N_6Se_4CeSb$	$C_8H_{26}N_6Se_4NdSb$	$C_8H_{26}N_6Se_4SmSb$
Formula weight	1646.94	784.05	788.18	794.29
Cryst syst	Triclinic	Orthorhombic	Monoclinic	Monoclinic
Space group	$P-1$	$P2_12_12_1$	$P2_1/n$	$P2_1/c$
a (Å)	10.107(2)	8.9653(7)	14.307(2)	10.1777(12)
b (Å)	12.069(3)	11.3985(8)	9.0127(12)	13.4837(15)
c (Å)	17.180(4)	19.7211(13)	15.427(2)	14.7983(19)
α (deg)	89.202(11)	90	90	90
β (deg)	88.287(9)	90	100.775(2)	98.744(3)
γ (deg)	87.139(11)	90	90	90
V (Å^3)	2092.0(9)	2015.3(2)	1954.2(5)	2007.2(4)
Z	2	4	4	4
T (K)	293(2)	223(2)	223(2)	223(2)
$D_{calcd.}$ (g cm^{-3})	2.615	2.584	2.679	2.628
Total, unique data	17,890, 6815	8692, 3666	12,061, 4452	9724, 3516
Parameters	295	183	182	182
R_1 ($I>2\sigma$ (I))	0.0788	0.0250	0.0260	0.0253
wR_2 (all data)	0.1975	0.0452	0.0537	0.0457
GOF on F^2	1.096	1.063	1.003	1.095

Anal. Found: C 11.52, H 3.43, N 11.53. Calcd. for $C_{16}H_{58}N_{14}Se_8Dy_2Sb_2$ (**2c**, 1646.94): C 11.67, H 3.55, N 11.67%.

2.3. Synthesis of $[Ln(en)(trien)(\mu\text{-}\eta^1,\eta^2\text{-}SbSe_4)]_\infty$ (*Ln*=Ce(**3a**), Nd(**3b**)) and $[Sm(en)(trien)(\eta^2\text{-}SbSe_4)]$ (**4a**)

$CeCl_3$ (123 mg, 0.5 mmol), Sb (61 mg, 0.25 mmol), Se (158 mg, 2 mmol), and 2 mL of a mixed en/trien (1:1(v/v)) solvent were loaded into a Teflon-lined stainless steel autoclave with an inner volume of 15 mL. The reaction was run at 180 °C for 6 days, then cooled to ambient temperature. Orange–yellow prism crystals of **3a** were filtered off, washed with ethanol and stored under a vacuum (65% yield based on Sb). Red crystals of **3b** (62% yield) and **4a** (66% yield) were prepared with a procedure similar to that for the synthesis of **3a**, except that Nd_2O_3 and Sm_2O_3 were used instead of $CeCl_3$, respectively. Anal. Found: C 12.13, H 3.36, N 10.66. Calcd. for $C_8H_{26}N_6Se_4LaSb$ (**3a**, 784.05): C 12.27, H 3.35, N 10.74%. Anal. Found: C 12.03, H 3.22, N 10.56. Calcd. for $C_8H_{26}N_6Se_4NdSb$ (**3b**, 788.18): C 12.19, H 3.32, N 10.66%. Anal. Found: C 12.01, H 3.25, N 10.43. Calcd. for $C_8H_{26}N_6Se_4SmSb$ (**4a**, 794.29): C 12.10, H 3.30, N 10.58%.

2.4. X-ray structure determination

All data were collected on a Rigaku Mercury CCD diffractometer with the exception of **2c**, **3a**, **3b** and **3c** on a Rigaku Saturn CCD diffractometer, using graphite-monochromated Mo-$K\alpha$ radiation with a ω-scanning mode to the maximum 2θ between 49.00° (**2c**) and 55.00° (**1a**). An empirical absorption correction was applied to the data. The structures were solved with SHELXS-97 [22], and refinement was performed against F^2 using SHELXL-97 [22]. All the non-hydrogen atoms were refined anisotropically. Atoms C(11) in **2a**, C(12) in **2b** and C(9) in **2c** are disordered and the occupancies are refined as 54% and 46%, 50% and 50%, 60% and 40%, respectively. H atoms were geometrically positioned and refined using the riding model. Technical details of data collections and refinement are summarized in Table 1.

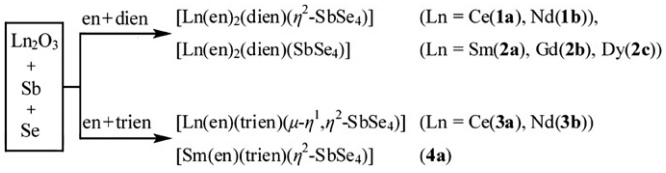

Scheme 1. Syntheses of **1a**–**4a**.

3. Results and discussion

3.1. Syntheses

The title complexes were prepared by the reactions of Ln_2O_3 ($CeCl_3$ for **1a** and **3a**), Sb and Se at 180 °C for 6 days in 1:1(v/v) mixed en/dien and en/trien solvents, respectively (Scheme 1). Under solvothermal conditions, the lanthanide oxides react in situ to form the mixed-coordinated $[Ln(en)_2(dien)]^{3+}$ and $[Ln(en)(trien)]^{3+}$ complex cations. The cations were coordinated by $[SbSe_4]^{3-}$ anions to generate neutral lanthanide complexes **1a**–**2c** and **3a**–**4a,** respectively. But the Ln_2O_3, Sb and Se reactions from Tb_2O_3 on in en/dien and from Gd_2O_3 on in en/trien across the lanthanide series yielded the Ln^{3+}-en complexes with the same general formula $[Ln(en)_4]SbSe_4 \cdot 0.5en$, which are isostructural with the compounds synthesized in the single en solvent several years ago [19]. The dien and trien ligands do not take part in the coordination to these lanthanides in the reactions. The Ln^{3+} ion size influences the formation of lanthanide complexes with the en/dien and en/trien mixed ligands. This work has shown that the solvothermal reaction of Ln_2O_3 in mixed polyamine solvents is an convenient and effective method to prepare Ln complexes with mixed ethylene polyamine ligands for the Ln^{3+} metals with larger ionic radius.

3.2. Structures of **1a**–**1b** and **2a**–**2c**

Complexes **1a** and **1b** crystallize in the monoclinic space group $P2_1/n$ with four formula units in the unit cell, and they are isostructural with the La^{3+} analog $[La(en)_2(dien)(\eta^2\text{-}SbSe_4)]$ (**1**) [20]. The crystal structure of **1a** is depicted in Fig. 1. Both Ce^{3+} and Nd^{3+} ions are coordinated by two bidentate en ligands, and one tridentate dien ligand, forming seven-coordinate complex cations $[Ln(en)_2(dien)]^{3+}$ (*Ln*=Ce, Nd). The $[SbSe_4]^{3-}$ anion acts as a bidentate η^2-$SbSe_4$ chelating ligand with Se(1) and Se(2) atoms to coordinate to $[Ln(en)_2(dien)]^{3+}$, resulting in the neutral complexes $[Ln(en)_2(dien)(\eta^2\text{-}SbSe_4)]$ (Fig. 1(a)). The Ln^{3+} ions are ninefold coordinated in a distorted monocapped square antiprismatic environment. (Fig. 1(b)). The Ln–Se [av. Ce–Se=3.1775(7) Å, Nd–Se=3.1384(9) Å] and Ln–N bond lengths [av. Ce–N=2.712(4) Å, Nd–N=2.657(6) Å] (Table 2) are consistent with corresponding bond lengths observed in literature [23–26], and decrease from Ce to Nd due to the lanthanide contraction. The Sb atom is coordinated by four Se atoms, forming a distorted tetrahedron with Sb–Se lengths in the range of 2.4555(15)–2.4886(8) Å and the Se–Sb–Se angles in the range of 101.73(5)°–114.11(6)° (Table 2) in agreement with literature data [11,27]. In **1a** and **1b** the $[Ln(en)_2(dien)(\eta^2\text{-}SbSe_4)]$ molecules are linked end-to-end via hydrogen bonding between

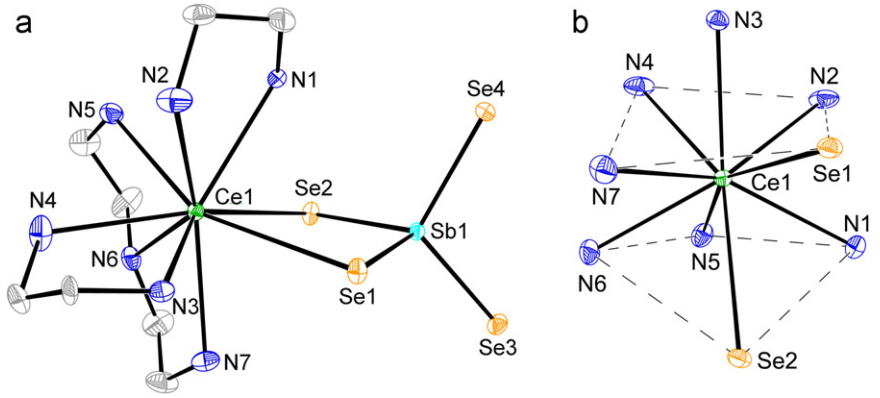

Fig. 1. (a) Crystal structure of **1a** with the labeling scheme (thermal ellipsoids are drawn at 30% probability). The hydrogen atoms are omitted for clarity. (b) Crystal structure of polyhedron CeN_7Se_2 in **1a**.

Table 2
Selected bond lengths (Å) and angles (deg) for **1a**–**4a**.

	1a (*Ln*=Ce)	**1b** (*Ln*=Nd)	**2a** (*Ln*=Sm)	**2b** (*Ln*=Gd)
Sb–Se	2.4589(7)–2.4886(8)	2.4563(10)–2.4851(9)	2.422(2)–2.498(2)	2.451(3)–2.459(3)
Ln–Se	3.1615(7), 3.1935(8)	3.1188(9), 3.1581(9)	3.004(2), 3.026(2)	3.006(3), 3.021(3)
Ln–N	2.680(5)–2.748(5)	2.620(6)–2.691(6)	2.478(14)–2.581(18)	2.50(2)–2.60(2)
Se–Sb–Se	102.52(2)–113.58(3)	101.75(3)–114.05(4)	103.24(8)–114.45(9)	103.26(10)–114.33(12)
Sb–Se(1)–Ln	90.36(2)	90.82(3)	119.59(7)	124.10(10)
Sb–Se(2)–Ln[a]	89.318(19)	89.60(2)	124.15(7)	120.08(9)
Se–Ln–Se	75.007(17)	75.50(2)		
N–Ln–Se	68.02(10)–154.09(11)	68.18(12)–152.77(15)	72.8(4)–152.2(4)	73.2(5)–152.2(5)
N–Ln–N	61.88(15)–142.70(15)	62.0(2)–143.3(2)	64.3(5)–145.0(5)	65.0(7)–145.4(7)
0.5				
	2c (*Ln*=Dy)	**3a** (*Ln*=Ce)	**3b** (*Ln*=Nd)	**4a** (*Ln*=Sm)
Sb–Se	2.430(5)–2.502(4)	2.4549(6)–2.4700(6)	2.4571(6)–2.4712(6)	2.4330(6)–2.4816(6)
Ln–Se	2.980(4), 2.997(4)	3.1834(7)–3.3091(6)	3.1727(6)–3.3044(6)	3.0059(6), 3.0553(6)
Ln–N	2.43(3)–2.56(3)	2.656(4)–2.717(4)	2.579(3)–2.643(4)	2.557(4)–2.592(4)
Se–Sb–Se	103.26(14)–114.43(19)	103.78(2)–112.06(3)	102.41(2)–113.34(2)	99.79(2)–113.35(2)
Sb–Se(1)–Ln	120.35(13)	89.307(19)	89.590(17)	91.323(18)
Sb–Se(2)–Ln[a]	124.34(14)	90.233(19)	89.622(17)	90.230(18)
Sb–Se(3)–Ln		117.83(2)	120.79(2)	
Se–Ln–Se		74.505(15)–137.819(19)	74.434(16)–137.159(14)	77.492(16)
N–Ln–Se	72.8(8)–151.6(7)	66.36(11)–143.35(11)	65.97(8)–147.74(8)	69.61(8)–147.34(9)
N–Ln–N	65.4(10)–145.5(10)	62.88(14)–149.18(14)	64.34(12)–147.87(12)	65.56(12)–159.53(13)

[a] Refer to the Sb–Se(5)–Ln angle in **2a**–**2c**.

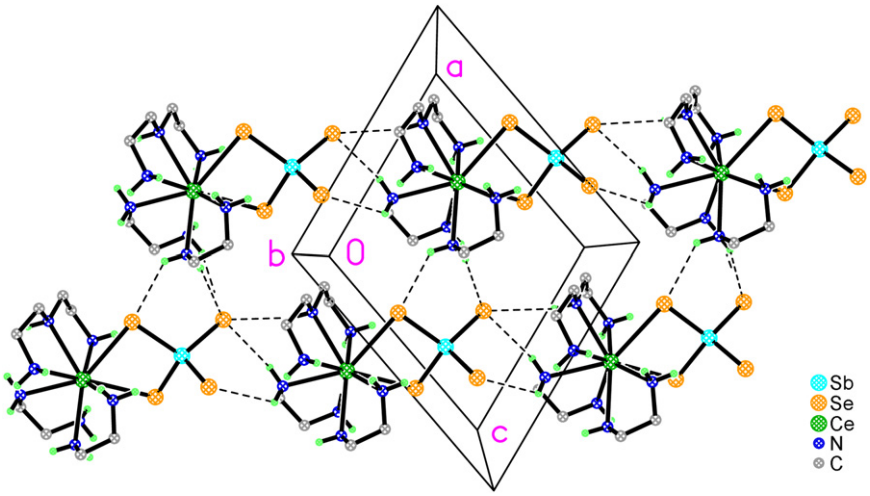

Fig. 2. A view of the layer constructed by the [Ce(en)$_2$(dien)(η^2-SbSe$_4$)] moieties via N–H···Se interactions (shown in dashed lines) in **1a**.

amino group and Se atoms to form a chain-like structure. Adjacent chains are linked through further N–H···Se interactions into layers perpendicular to the *b* axis (Fig. 2), and then, the layers are connected into a 3-D supramolecular network via the N–H···Se bonds (Fig. S1 in the Supplementary material).

Complexes **2a**–**2c** are isostructural with general formula [*Ln*(en)$_2$(dien)(SbSe$_4$)]$_2$ (*Ln*=Sm(**2a**), Gd(**2b**), Dy(**2c**)) (Table 1). There are two crystallographically independent [*Ln*(en)$_2$(dien)(SbSe$_4$)] moieties in **2a**–**2c**. Both Ln^{3+}(1) and Ln^{3+}(2) ions are coordinated by two bidentate en, one tridentate dien and one monodentate [SbSe$_4$]$^{3-}$ ligands, forming the mixed-coordinated neutral complex [*Ln*(en)$_2$(dien)(SbSe$_4$)]. The structure of [Sm(1)(en)$_2$(dien)(Sb(1)Se$_4$)] in **2a** is depicted in Fig. 3(a). Both Ln^{3+}(1) and Ln^{3+}(2) are in eight-fold coordination environments and form bicapped trigonal prisms (Fig. 3(b)). The [*Ln*(1)(en)$_2$(dien)(Sb(1)Se$_4$)] and [*Ln*(2)(en)$_2$(dien)(Sb(2)Se$_4$)] moieties exhibit very similar molecular structures except that the former possesses a smaller Ln–Se–Sb angle than the latter (Table 2). The Ln–N and Ln–Se bond lengths of **2a**–**2c** (Table 2) are in the range of the literature values, respectively [19,20,24,28]. In **2a**–**2c**, the tetrahedral [SbSe$_4$]$^{3-}$ anion acts as a monodentate ligand to the Ln^{3+} ions. The Sb–Se lengths and Se–Sb–Se angles agree with those of the corresponding values in **1a** and **1b** (Table 2). In **2a**–**2c**, the complexes are alternatively connected end to end into an one-dimensional chain parallel to the *c* axis (Fig. 4) through N–H···Se contacts with N···Se separations between 3.412(16) and 3.68(2) Å and corresponding N–H···Se angles between 142.4° and 167.0°, indicating weak hydrogen bonds. The chains are linked into a 3-D H-bonded network via further N–H···Se bonds (Fig. S2 in the Supplementary material).

3.3. *Structures of **3a**, **3b** and **4a***

Complexes **3a** and **3b** crystallize in orthorhombic and monoclinic crystal system, respectively, but they display the same structure. The Ce^{3+} and Nd^{3+} ions are coordinated by a bidentate en and a tetradentate trien ligands, forming six-coordinate complex cations [*Ln*(en)(trien)]$^{3+}$ (*Ln*=Ce, Nd). The [SbSe$_4$]$^{3-}$ anion

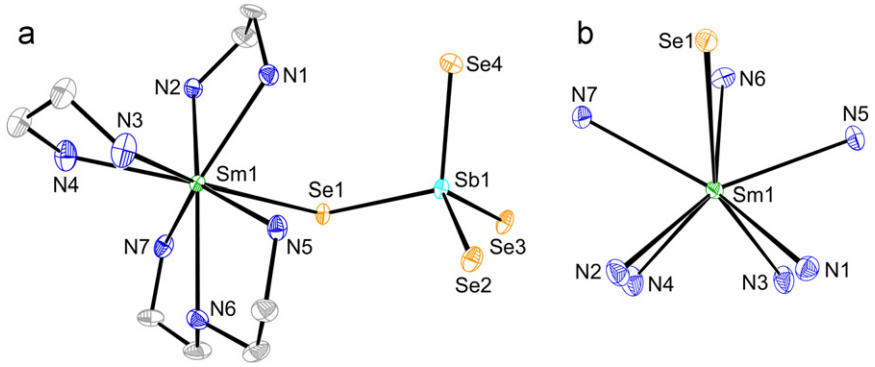

Fig. 3. (a) Crystal structure of the $[Sm(1)(en)_2(dien)(Sb(1)Se_4)]$ moiety in **2a** with the labeling scheme (thermal ellipsoids are drawn at 30% probability). The hydrogen atoms are omitted for clarity. (b) Crystal structure of polyhedron SmN_7Se in **2a**.

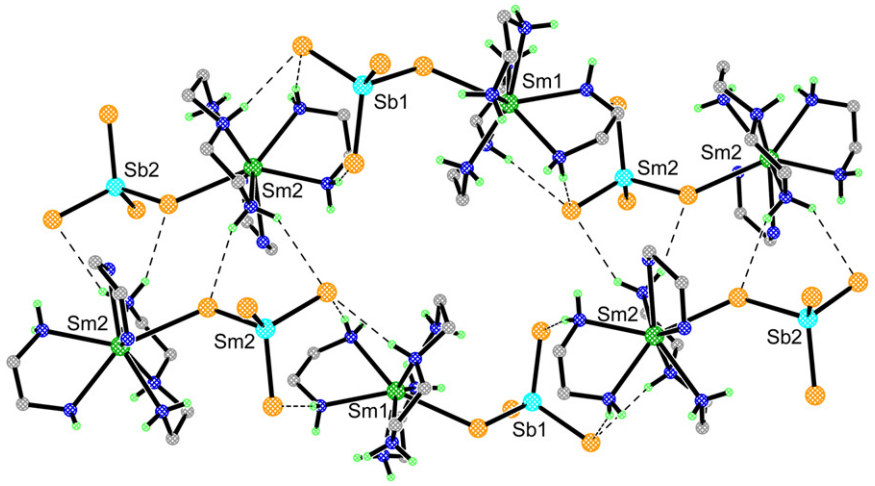

Fig. 4. A view of the layer constructed by the $[Sm(1)(en)_2(dien)(Sb(1)Se_4)]$ and $[Sm(2)(en)_2(dien)(Sb(2)Se_4)]$ moieties via N–H···Se interactions (shown in dashed lines) in **2a**.

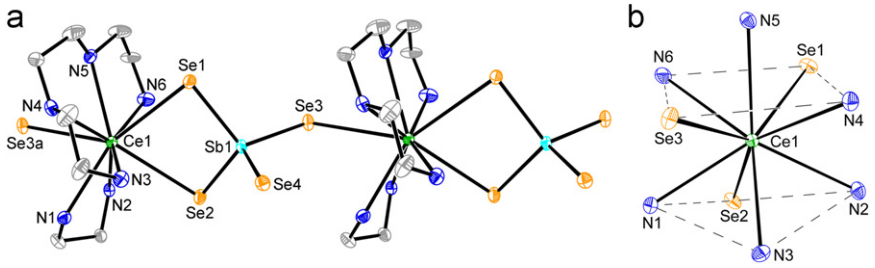

Fig. 5. Crystal structure of **3a** with the labeling scheme (thermal ellipsoids are drawn at 30% probability). The hydrogen atoms are omitted for clarity.

acts as a tridentate μ-η^1,η^2-$SbSe_4$ bridging ligand with Se(1), Se(2) and Se(3) atoms to link the $[Ln(en)(trien)]^{3+}$ cations into neutral coordination polymer $[Ln(en)(trien)(\mu\text{-}\eta^1,\eta^2\text{-}SbSe_4)]_\infty$ (Fig. 5). The Sb–Se lengths and the Se–Sb–Se angles are in the range of the corresponding values in **1a** and **1b** (Table 1). The Ln^{3+} ions are coordinated by six N atoms and three Se atoms forming distorted monocapped square antiprisms LnN_6Se_3 as the CeN_7Se_2 polyhedron in **1a**. In **3a**, the bond lengths of Ce–Se(1) [3.2254(7) Å], Ce–Se(2) [3.1834(7) Å] and Ce–N [av. Ce–N = 2.690(4) Å] (Table 2) are comparable to those of **1a**, except Ce–Se(3) [3.3091(6) Å] being slightly longer. The same Nd–Se and Nd–N bond length evolution is observed between **1b** and **3b**. In the crystal structures of **3a** and **3b**, the $[Ln(en)(trien)(\mu\text{-}\eta^1,\eta^2\text{-}SbSe_4)]_\infty$ chains interact with neighbors via N–H···Se hydrogen bonding, generating a layer perpendicular to the *c* axis (Fig. 6). The layers are linked into a 3-D H-bonding network via addition N–H···Se hydrogen bonds (Fig. S3 in the Supplementary material).

Complex **4a** crystallizes in the monoclinic space group $P2_1/c$ with four formula units in the unit cell. It is isostructural with $[Eu(en)(trien)(\eta^2\text{-}SbSe_4)]$ (**4**) [20]. The crystal structure of **4a** is depicted in Fig. 7. The Sm^{3+} ion is coordinated by one bidentate en, and one tetradentate trien ligands, yielding the six-coordinated complex. Like the $[SbSe_4]^{3-}$ anions in **1a** and **1b**, the $[SbSe_4]^{3-}$ anion in **4a** also acts in a η^2-fashion chelating the Sm^{3+} ion via Se(1) and Se(2), leading to the neutral complex $[Sm(en)(trien)(\eta^2\text{-}SbSe_4)]$ (Fig. 7). The Sm^{3+} ion is in a bicapped trigonal prismatic environment like Sm^{3+} ion in **2a**. The average Sm–Se and Sm–N bond lengths are 3.0306(6) and 2.569(4) Å, respectively, (Table 2), which are in the range of the corresponding values obtained for **2a**.

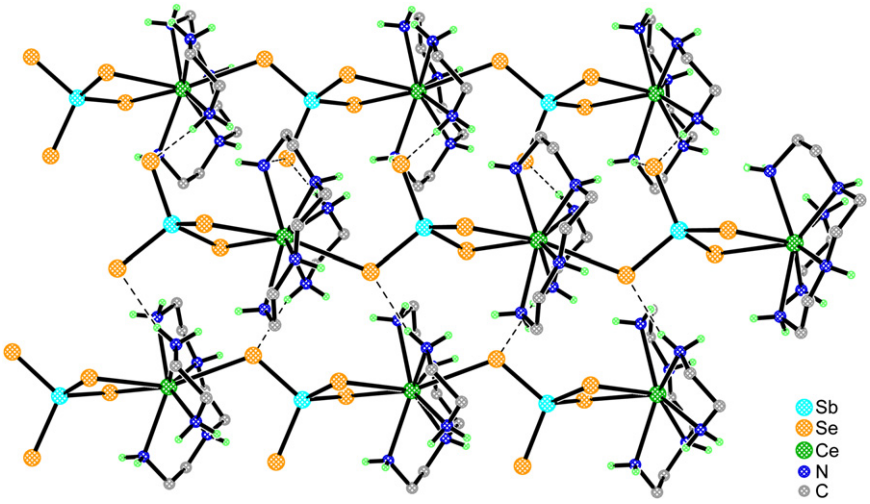

Fig. 6. A view of the layer constructed by the $[Ce(en)(trien)(\mu\text{-}\eta^1,\eta^2\text{-}SbSe_4)]_\infty$ chains via N–H···Se interactions (shown in dashed lines) in **3a**.

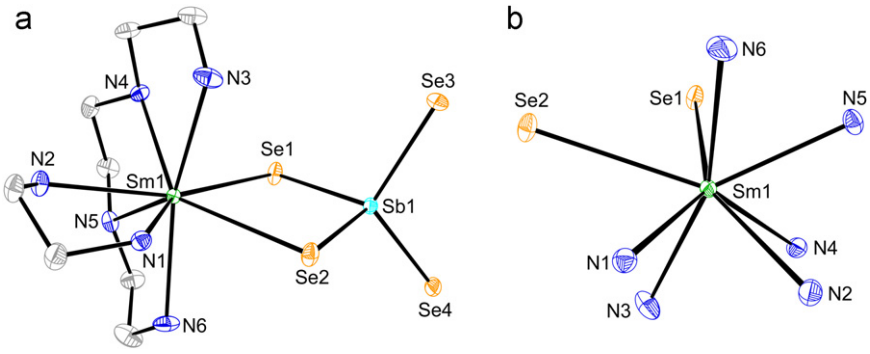

Fig. 7. Crystal structure of **4a** with the labeling scheme (thermal ellipsoids are drawn at 30% probability). The hydrogen atoms are omitted for clarity.

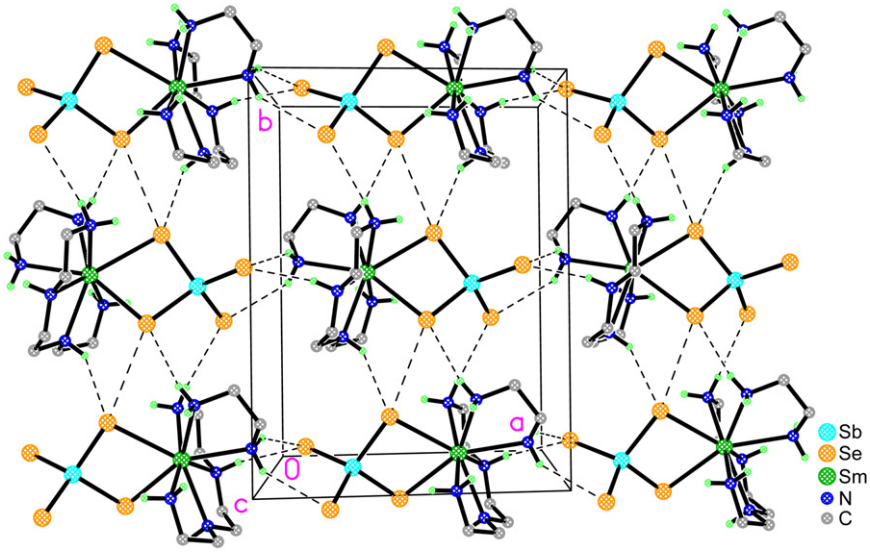

Fig. 8. A view of the layer constructed by the $[Sm(en)(trien)(\eta^2\text{-}SbSe_4)]$ molecules via N–H···Se interactions (shown in dashed lines) in **4a**.

The $[Sm(en)(trien)(\eta^2\text{-}SbSe_4)]$ molecules are connected end to end into one dimensional chains via N–H···Se H-bonding, and the chains are further connected into a layer parallel to the (0 0 1) plane of the unit cell by hydrogen bonds (Fig. 8). The orientations of the chains alternate in the same layer. The layers are linked into a 3-D H-bonding network via further N–H···Se bonds (Fig. S4 in the Supplementary material).

3.4. Lanthanide contraction effect on the structures of [Ln(en)$_2$(dien)(SbSe$_4$)] and [Ln(en)(trien) (SbSe$_4$)] series.

The $[SbSe_4]^{3-}$ and $[Ln(en)_2(dien)]^{3+}$ ions form two structural types across the lanthanide series. The $[SbSe_4]^{3-}$ coordinate to $[Ln(en)_2(dien)]^{3+}$ as a η^2-$SbSe_4$ ligand from La^{3+} to Nd^{3+} and acts as a mono-$SbSe_4$ ligand from Sm^{3+} to Dy^{3+}, giving complexes

[*Ln*(en)$_2$(dien)(η^2-SbSe$_4$)] (*Ln*=La(**1**),[20] Ce(**1a**), Nd(**1b**)) and [*Ln*(en)$_2$(dien)(SbSe$_4$)] (*Ln*=Sm(**2a**), Gd(**2b**), Dy(**2c**)), respectively. The [*Ln*(en)(trien)(SbSe$_4$)] series also possess [*Ln*(en)(trien)(μ-η^1,η^2-SbSe$_4$)]$_\infty$(*Ln*=La(**3**) [20], Ce(**3a**), Nd(**3b**)) and [*Ln*(en)(trien)(η^2-SbSe$_4$)] (*Ln*=Eu(**4**) [20], Sm(**4a**)) two structural types, in which μ-η^1,η^2-SbSe$_4$ and η^2-SbSe$_4$ coordination modes are observed for the $[SbSe_4]^{3-}$ anions. Apparently, the structural evolution in the two series is related with the Ln^{3+} ion size. The ionic radii of the Ln^{3+} ions decrease monotonously from La^{3+} to Lu^{3+} due to lanthanide contraction effect, therefore, the coordination numbers of Ln^{3+} ions prefer nine for lighter lanthanide ions and eight for the heavier ones [29]. To maintain a coordination number of nine for $La^{3+}-Nd^{3+}$, the $[SbSe_4]^{3-}$ anion coordinates to seven-coordinate [*Ln*(en)$_2$(dien)]$^{3+}$ and six-coordinate [*Ln*(en)(trien)]$^{3+}$ as bidentate η^2-SbSe$_4$ and tridentate μ-η^1,η^2-SbSe$_4$ ligands, and [*Ln*(en)$_2$(dien)(η^2-SbSe$_4$)] (**1**, **1a**, and **1b**) and [*Ln*(en)(trien)(μ-η^1,η^2-SbSe$_4$)]$_\infty$ (**3**, **3a**, and **3b**) are obtained, respectively. From Sm on, the $[SbSe_4]^{3-}$ anion coordinates to [*Ln*(en)$_2$(dien)]$^{3+}$ and [*Ln*(en)(trien)]$^{3+}$ as *mono*-SbSe$_4$ and η^2-SbSe$_4$ to satisfy coordination number of eight for the Ln^{3+} ions, generating [*Ln*(en)$_2$(dien)(η^2-SbSe$_4$)] (**2a**, **2b**, and **2c**) and [*Ln*(en)(trien)(η^2-SbSe$_4$)] (**4** and **4a**), respectively.

3.5. Optical properties

Solid state optical absorption spectra of complexes **1a**–**4a** were recorded from powder samples at room temperature, and the representative spectra of cerium (**1a** and **3a**) and samarium (**2a** and **4a**) complexes are shown in Fig. 9(a) and (b). The complexes exhibit well-defined steep absorption edges from which the band gaps (E_g) can be estimated as 2.51, 2.13, 2.21, 2.19, 2.14, 2.38, 2.09, and 2.08 eV for **1a**−**4a**, indicating semiconducting properties of the title complexes. The band gaps are much larger than those of the layered copper selenidoantimonates $Cs_2Cu_2Sb_2Se_5$ (1.2−1.3 eV) [30], $Cu_2SbSe_3\cdot 0.5en$ (1.58 eV) [31], and $Cu_2SbSe_3\cdot en$ (1.61 eV) [31]. The electronic transitions are likely results of charge transfer from the Se^{2-}-dominated valence band to the Ln^{3+}-dominated conduction band, as occurred in the multinary chalcogenometalates [32].

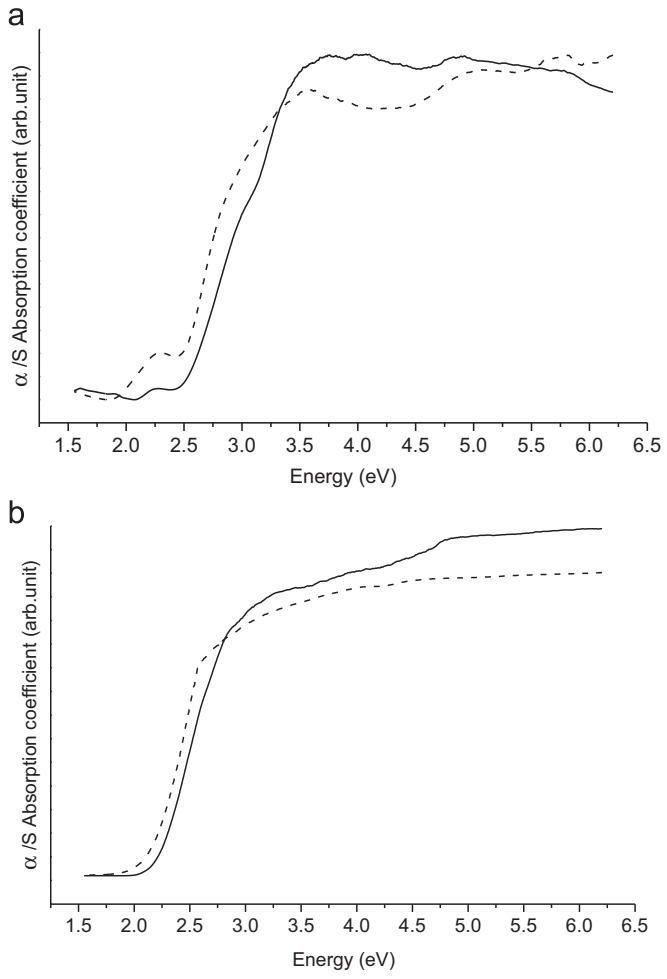

Fig. 9. Solid state optical absorption spectra for (a) **1a** (solid line) and **3a** (dashed line); (b) **2a** (solid line) and **4a** (dashed line).

4. Conclusion

In conclusion, we have successfully achieved the coordination of the soft base ligand $[SbSe_4]^{3-}$ to the lanthanide(III) centers by using en+dien and en+tren mixed polyamines as co-ligands. Investigation of the mixed polyamine systems Ln/Sb/Se/(en+dien) and Ln/Sb/Se/(en+trien) reveals that two structural types of lanthanide(III) selenidoantimonates are formed across lanthanide series for the two systems. The structural turnover of two structural types occurs at Sm for both systems. The structural evolution along the lanthanide series is attributed to lanthanide contraction effect. In addition, the syntheses and characterizations of the title complexes show that the coordination of $[SbSe_4]^{3-}$ anion to the same lanthanide(III) ion can also be controlled by en/dien and en/trien mixed polyamines beside by the single polyamine [19].

Acknowledgments

This work was supported by the National Natural Science Foundation of P. R. China (No. 20771077), and the Key Laboratory of Organic Synthesis of Jiangsu Province.

Appendix A. Supplementary material

Supplementary data associated with this article can be found in the online version at doi:10.1016/j.jssc.2011.03.039.

Crystallographic data for the structures reported in this paper have been deposited with the Cambridge Crystallographic Data Centre as supplementary publication number no. CCDC 782813 (**1a**), 782814 (**1b**), 782815 (**2a**), 782816 (**2b**), 782817 (**2c**), 782818 (**3a**), 782819 (**3b**), and 782820 (**4a**) Copies of the data can be obtained free of charge on application to CCDC, 12 Union Road, Cambridge CB2 1EZ, UK (fax: (44) 1223 336-033; e-mail: deposit@ccdc.cam.ac.uk).

References

[1] (a) J. Li, Z. Chen, R.J. Wang, D.M. Proserpio, Coord. Chem. Rev. 190–192 (1999) 707–735;
(b) W.S. Sheldrick, M. Wachhold, Coord. Chem. Rev. 176 (1998) 211–322;
(c) Z. Chen, R.-J. Wang, J. Li, Chem. Mater. 12 (2000) 762–766;
(d) T. Van. Almsick, A. Loose, W.S. Sheldrick, Z. Anorg. Allg. Chem. 631 (2005) 21–23;
(e) D.X. Jia, J. Dai, Q.Y. Zhu, L.H. Cao, H.H. Lin, J. Solid State Chem. 178 (2005) 874–881;
(f) D.X. Jia, A.M. Zhu, Y. Zhang, J. Deng, Monatsh. Chem. 138 (2007) 191–197.
[2] (a) J.L. Shreeve-Keyer, C.J. Warren, S.S. Dhingra, R.C. Haushalter, Polyhedron 16 (1997) 1193–1199;
(b) J. Li, Z. Chen, T.J. Emge, T. Yuen, D.M. Proserpio, Inorg. Chim. Acta. 273 (1998) 310–315;
(c) D.X. Jia, Y. Zhang, J. Dai, Q.Y. Zhu, X.M. Gu, Z. Anorg. Allg. Chem. 630 (2004) 313–318;

(d) D.X. Jia, J. Dai, Q.Y. Zhu, Y. Zhang, X.M. Gu, Polyhedron 23 (2004) 937–942.
[3] (a) J.-H. Chou, M.G. Kanatzidis, Inorg. Chem. 33 (1994) 5372–5373;
(b) J.-H. Chou, M.G. Kanatzidis, Chem. Mater. 7 (1995) 5–8;
(c) M.G. Kanatzidis, J.-H. Chou, J. Solid State Chem. 127 (1996) 186–201;
(d) J.-H. Chou, J.A. Hanko, M.G. Kanatzidis, Inorg. Chem. 36 (1997) 4–9;
(e) M. Wachhold, M.G. Kanatzidis, Inorg. Chem. 38 (1999) 4178–4180;
(f) R.G. Iyer, M.G. Kanatzidis, Inorg. Chem. 41 (2002) 3605–3607;
(g) M.L. Fu, G.C. Guo, X. Liu, B. Liu, L.Z. Cai, J.S. Huang, Inorg. Chem. Commun. 8 (2005) 18–21;
(h) X. Wang, T.-L. Sheng, S.-M. Hua, R.-B. Fu, J.-S. Chen, X.-T. Wu, J. Solid State Chem. 182 (2009) 913–919.
[4] (a) H.O. Stephan, M.G. Kanatzidis, J. Am. Chem. Soc. 118 (1996) 12226–12227;
(b) H.O. Stephan, M.G. Kanatzidis, Inorg. Chem. 36 (1997) 6050–6057;
(c) W. Bensch, C. Näther, R. Stähler, Chem. Commun. (2001) 477–478;
(d) R. Stähler, C. Näther, W. Bensch, Eur. J. Inorg. Chem. (2001) 1835–1840;
(e) A.V. Powell, R. Paniagua, P. Vaqueiro, A.M. Chippindale, Chem. Mater. 14 (2002) 1220–1224;
(f) R. Stähler, B.D. Mosel, H. Eckert, W. Bensch, Angew. Chem. Int. Ed. 41 (2002) 4487–4489;
(g) R. Stähler, C. Näther, W. Bensch, J. Solid State Chem. 174 (2003) 264–275;
(h) R. Kiebach, F. Studt, C. Näther, W. Bensch, Eur. J. Inorg. Chem. (2004) 2553–2556;
(i) P. Vaqueiro, A.M. Chippindale, A.V. Powell, Inorg. Chem. 43 (2004) 7963–7965;
(j) P. Vaqueiro, D.P. Darlow, A.V. Powell, A.M. Chippindale, Solid State Ion. 172 (2004) 601–605;
(k) D.X. Jia, Y. Zhang, Q.X. Zhao, J. Deng, Inorg. Chem. 45 (2006) 9812–9817;
(l) A. Puls, C. Näther, W. Bensch, Z. Anorg. Allg. Chem. 632 (2006) 1239–1243.
[5] M. Melullis, M.K. Brandmayer, S. Dehnen, Z. Anorg. Allg. Chem. 632 (2006) 64–72.
[6] X.M. Gu, J. Dai, D.X. Jia, Y. Zhang, Q.Y. Zhu, Cryst. Growth Des. 5 (2005) 1845–1848.
[7] M.L. Fu, G.C. Guo, L.Z. Cai, Z.J. Zhang, J.S. Huang, Inorg. Chem. 44 (2005) 184–186.
[8] M. Schur, H. Rijnberk, C. Näther, W. Bensch, Polyhedron. 18 (1998) 101–107.
[9] M. Schur, W. Bensch, Z. Naturforsch. B57 (2002) 1–7.
[10] L. Engelke, R. Stähler, M. Schur, C. Näther, W. Bensch, R. Pöttgen, M.H. Möller, Z. Naturforsch. B59 (2004) 869–876.
[11] W. Bensch, C. Näther, M. Schur, Chem. Commun. (1997) 1773–1774.
[12] T. van Almsick, W.S. Sheldrick, Z. Anorg. Allg. Chem. 632 (2006) 1413–1415.
[13] (a) M. Behrens, S. Scherb, C. Näther, W. Bensch, Z. Anorg. Allg. Chem. 629 (2003) 1367–1373;
(b) R. Stähler, W. Bensch, Eur. J. Inorg. Chem. (2001) 3073–3078;
(c) R. Stähler, W. Bensch, J. Chem. Soc. Dalton Trans. (2001) 2518–2522;
(d) R. Kiebach, W. Bensch, R.-D. Hoffmann, R. Pöttgen, Z. Anorg. Allg. Chem. 629 (2003) 532–538;
(e) M. Schaefer, C. Näther, W. Bensch, Solid State Sci. 5 (2003) 1135–1139;
(f) M. Schaefer, R. Stähler, W.R. Kiebach, C. Näther, W. Bensch, Z. Anorg. Allg. Chem. 630 (2004) 1816–1822;
(g) M. Schaefer, C. Näther, N. Lehnert, W. Bensch, Inorg. Chem. 43 (2004) 2914–2921;
(h) M. Schaefer, D. Kurowski, A. Pfitzner, C. Näther, Z. Rejai, K. Möller, N. Ziegler, W. Bensch, Inorg. Chem. 45 (2006) 3726–3731;
(i) K. Möller, C. Näther, A. Bannwarth, W. Bensch, Z. Anorg. Allg. Chem. 633 (2007) 2635–2640;
(j) H. Lühmann, Z. Rejai, K. Möller, P. Leisner, M.-E. Ordolff, C. Näther, W. Bensch, Z. Anorg. Allg. Chem. 634 (2008) 1687–1695;
(k) L. Engelke, C. Näther, P. Leisner, W. Bensch, Z. Anorg. Allg. Chem. 634 (2008) 2959–2965;
(l) A. Kromm, W.S. Sheldrick, Z. Anorg. Allg. Chem. 634 (2008) 121–124;
(m) A. Kromm, W.S. Sheldrick, Z. Anorg. Allg. Chem. 634 (2008) 225–227;
(n) A. Kromm, W.S. Sheldrick, Z. Anorg. Allg. Chem. 635 (2009) 205–207.
[14] (a) N. Pienack, S. Lehmann, H. Lühmann, M. El-Madani, C. Näther, W. Bensch, Z. Anorg. Allg. Chem. 634 (2008) 2323–2329;
(b) J.F. Chen, Q.Y. Jin, Y.L. Pan, Y. Zhang, D.X. Jia, Z. Anorg. Allg. Chem. 636 (2010) 230–235.
[15] A. Cassol, P. Di Bernardo, R. Portanova, M. Tolazzi, G. Tomat, P. Zanonato, J. Chem. Soc. Dalton Trans. (1992) 469–474.
[16] (a) A.M. Zhu, Q.Y. Jin, D.X. Jia, J.S. Gu, Y. Zhang, Eur. J. Inorg. Chem. (2008) 4756–4761;
(b) J.F. Chen, Q.Y. Jin, Y.L. Pan, Y. Zhang, D.X. Jia, Chem. Commun. (2009) 7212–7214.
[17] D.X. Jia, A.M. Zhu, J. Deng, Y. Zhang, J. Dai, Dalton Trans. (2007) 2083–2086.
[18] (a) D.X. Jia, Q.Y. Zhu, J. Dai, W. Lu, W.J. Guo, Inorg. Chem. 44 (2005) 819–821;
(b) D.X. Jia, Q.X. Zhao, Y. Zhang, J. Dai, J.L. Zou, Inorg. Chem. 44 (2005) 8861–8867.
[19] (a) D.X. Jia, Q.X. Zhao, Y. Zhang, J. Dai, J. Zhou, Eur. J. Inorg. Chem. (2006) 2760–2765;
(b) D.X. Jia, A.M. Zhu, Q.Y. Jin, Y. Zhang, W.Q. Jiang, J. Solid State Chem. 181 (2008) 2370–2377.
[20] D.X. Jia, Q.Y. Jin, J.F. Chen, Y.L. Pan, Y. Zhang, Inorg. Chem. 48 (2009) 8286–8293.
[21] W.W. Wendlandt, H.G. Hecht, Reflectance Spectroscopy, Interscience Publishers, New York, 1966.
[22] (a) G.M. Sheldrick, SHELXS-97, Program for Crystal Structure Determination, University of Göttingen, Germany, 1997;
(b) G.M. Sheldrick, SHELXL-97, Program for the Refinement of Crystal Structures, University of Göttingen, Germany, 1997.
[23] I. Ijjaali, K. Mitchell, J.A. Ibers, J. Solid State Chem. 177 (2004) 760–764.
[24] I. Ijjaali, B. Deng, J.A. Ibers, J. Solid State Chem. 178 (2005) 1503 – 1507.
[25] K. Muller-Buschbaum, C.C. Quitmann, Inorg. Chem. 45 (2006) 2678 – 2687.
[26] (a) M.M. Essig, D.W. Keogh, B.L. Scott, J.G. Watkin, Polyhedron 20 (2001) 373–377;
(b) S.A. Cotton, V. Franckevicius, R.E. How, B. Ahrens, L.L. Ooi, M.F. Mahon, P.R. Raithby, S.J. Teat, Polyhedron 22 (2003) 1489–1497.
[27] (a) M.A. Pell, J.A. Ibers., Inorg. Chem. 35 (1996) 4559–4562;
(b) F. Wendland, C. Näther, M. Schur, W. Bensch, Acta Crystallogr. C54 (1998) 317–319;
(c) R. Blachnik, A. Fehlker, H. Reuter, Z. Kristallogr. 216 (2001) 211–212.
[28] K. Mitchell, C.L. Haynes, A.D. McFarland, R.P. Van Duyne, J.A. Ibers, Inorg. Chem. 41 (2002) 1199–1204.
[29] C. Cossy, A.C. Barnes, J.E. Enderby, A.E. Merbach, J. Chem. Phys. 90 (1989) 3254–3259.
[30] Z. Chen, R.J. Wang, K.J. Dilks, J. Li, J. Solid State Chem. 147 (1999) 132–139.
[31] Z. Chen, R.E. Dilks, R.J. Wang, J.Y. Lu, J. Li, Chem. Mater. 10 (1998) 3184–3188.
[32] (a) M.L. Fu, G.C. Guo, X. Liu, W.T. Chen, B. Liu, J.S. Huang, Inorg. Chem. 45 (2006) 5793–5798;
(b) X. Bu, N. Zheng, X. Wang, B. Wang, P. Feng, Angew. Chem. Int. Ed. 43 (2004) 1502–1505;
(c) T. Wu, X. Wang, X. Bu, X. Zhao, L. Wang, P. Feng, Angew. Chem. Int. Ed. 48 (2009) 7204–7207.